Engineering Science and Military Technologies
Volume (5) - Issue (2) - Sep 2021
ISSN: 2357- 0954
DOI:10.21608/EJMTC.2022.104230.1202

Parametric study of stresses affecting the external and internal fibers of connecting rod small end

Original Article

Mohamed I. Amin

Mechanical Power Department, Military Technical College, Egypt

Keywords:
Connecting rod, internal combustion engines, parametric study, small end.

Corresponding Author:
Mohamed I. Amin, Mechanical Power Department, Military Technical College, Egypt, **Email:** mamin@mtc.edu.eg

Abstract
Connecting rod is an important element in reciprocating engines which faces various stress conditions. For long time, extensive efforts are conducted to reduce its weight and consequently affecting inertia force and cost. The purpose of this work is to study the factors which control the stresses affecting external and internal surfaces of connecting rod small end.These stresses result from inertia force of piston group mass and part of connecting rod. The transient section between small end and shank is considered as the most critical sectionat angle φz. The value of internal stress is found to be zero at certain value of this angle.In this study, a comprehensive investigation has been conducted to study the effect of changing small end design parameters on the value of angle (φzo) at which internal stress equals zero. The results showed that there is no effect of inertia force and small end width, while small end thickness, mean radius, and load distribution factor have dominant effect on this angle value. By using regression, a new correlation between (φzo) and dominant design parameters has been introduced with maximum error 0.7%. Verification of analytical study has been conducted using ANSYS numerical analysis software.Such a relation could be a useful tool for engine designers to predict the value of (φzo) to be a guide to change small end dimensions and its material which participate in reduction of connecting rod weight and price.

1. INTRODUCTION

Connecting rod transmits the forces acting on the piston pin to the crank pin. The connecting rod small end moves in linear reciprocating motion, while the big one moves in a rotary motion.The design and shape of connecting rod small end depend mainly on piston pin size and how it is fastened to small end and piston bosses. The small end is loaded by gas pressure force, reciprocating inertia force, and pre-stressing caused by pressing-in the bush[1].

Extensive investigations have been conducted by researchers in past decades in attempt to specify critical and most loaded sections in connecting rods, and to suggest how to reduce its weight. To achieve their goal, researchers used different types of software packages for modeling and analyzing the results.Vivek and Dilip[2] used Finite Element and Ansys Workbench software then verified their results experimentally by Optical Method. They concludedthat high stress concentrations affect both small and big ends more than the shank, and the small end is much higher stressed than the big one. Therefore, failure could be happened at the section of both ends. Using ANSYS 15, Akbar H Khan[3] introduced the same conclusion as[2].Shriram and Burande[4] Performed a three dimensional finite element model for a cast iron connecting rod in PROE and ANSYS workbench for Analysis. They noticed that the stress decreases from small to big end, and the maximum stresses occurred at the transition section between shank and both ends. The fillet regions of both ends are also highly stressed. While, lower stresses occurred at the shank region of connecting rod. Anusha *et al.*[5] investigated two different materials by creating a connecting rod model using ANSYS. Model results show that there is a stress peak in small end region. Abhinav *et al.*[6] conducted a static stress analysis for a connecting rod model. They confirmed that the area near the root of the connecting rod's small end susceptible to failure.

Researchers concluded that it is a mandatory to reduce connecting rod weight which results in inertia force and stresses reduction, in addition to lower cost especially in mass production. Borse Rajendra *et. al.*[7] used ANSYS 9.0 to analyze and investigate how to reduce weight and cost for steel forged connecting rods. They concluded that using materials such as micro-alloyed steels which have higher yield strength and endurance limit, leads to small and big ends weight reduction. They concluded also hardening of parts which have higher stresses should have more attention during manufacturing stage for weight reduction. Nilam *et al.*[8], Magish *et al.*[9], Wankhade *et al.*[10],

and Mithilesh *et al.*[11] used ANSYS 15 for modeling and analyzing connecting rod stress for different materials. They suggested that using composite materials such as carbon fibers introduces promising results in weight reduction. Other authors like Adnan Ali *et al.*[12] recommended Titanium alloy for the same purpose.Strozzi *et. al.*[13], and authors[14-18] concluded that carful modification and optimization of connecting rod design parameters and shape, has a significant effect in weight reduction and stress improvement.

It is a major target for all researchers to reduce connecting rod weight, either by using different lighter materials than conventional ones, or by optimization of geometry and dimensions. This paper aims to investigate different parameters which affect the value of stresses presented in most critical section, namely the transition between small end and shank as mentioned in previous work. This investigation could be a new approach leads to stress reduction through changing some design parameters, hence dimensions and weight decrease. This study shows zero internal stress at small end critical section for a certain inclination angle value of this critical section relative to vertical axis, depending on small end geometry. Moreover a correlation between this angle value and other design parameters has been introduced, which could be a useful tool design for stress reduction and thus weight and cost.

2. PARAMETRIC STUDY

Small end of the connecting rod is loaded mainly by inertia forces resulted from the linear reciprocating motion of piston group. Section I-I shown in figure 1 is considered to be the critical section in small end because it is the transient one between shank and small end. To determine the stresses which act on external and internal fibers of this section due to inertia force, it is assumed that the small end is a fixed-fixed curved beam with circular shape of mean radius (r), and a fixed rectangular shape at the point of transition.

Then external and internal stresses affecting section I-I can be calculated from [1]:

$$\sigma_{ex} = \left[2M_s\left(\frac{6r+h}{h(2r+h)}\right) + kN_s\right]\frac{1}{ah} \qquad (1)$$

$$\sigma_{in} = \left[-2M_s\left(\frac{6r-h}{h(2r-h)}\right) + kN_s\right]\frac{1}{ah} \qquad (2)$$

Where, (a) and (h) are small end width and thickness, while Ms and Ns are the resultant moment and force acting on transient critical section I-I shown in figure 2, and equal to:

$M_s = M_{os} + N_{os}\, r\,(1- \cos\varphi_z) - 0.5\, F\, r\,(\sin\varphi_z - \cos\varphi_z)$ (3)

$N_s = Nos \cos\varphi_z + 0.5\, F\,(\sin\varphi_z - \cos\varphi_z)$ (4)

Mos and Nos are the bending moment and normal force at the middle section (0-0) (Figure 2) due to breaking the curved beam at the middle and rejecting its right part and replacing it by them. Mos and Nos are given by the empirical formulae [1]:

$M_{os} = F\, r\, [\,0.00033\, \varphi_z - 0.0297]$ (5)

$N_{os} = F\,[0.572 - 0.0008\, \varphi_z]$ (6)

r…...Mean radius = (D+d) / 4 (Figure 1) (7)

F…..Inertia force due to reciprocating mass.

φ_z…Angle at which critical section I-I is located. The angle is measured in degrees from the vertical axis counter clockwise and can be obtained from [1]:

$$\phi_z = 90^o + \cos^{-1}\left[\frac{H/2+\rho_1}{D/2+\rho_1}\right] \qquad (8)$$

D and d are the external and internal diameters of small end.

H is the width of shank just below the small end (Figure 1).

ρ1 is the curvature at the transition zone (Figure 1).

It is worth to notice that the force Ns and the moment Ms are acting on both connecting rod and bush, k is the stress distribution coefficient and equals:

$K = EA/(EA+E_bAb]$

E_b and E Young's modulus of bush and small end.

A_b and A Cross section areas of bush and small end.

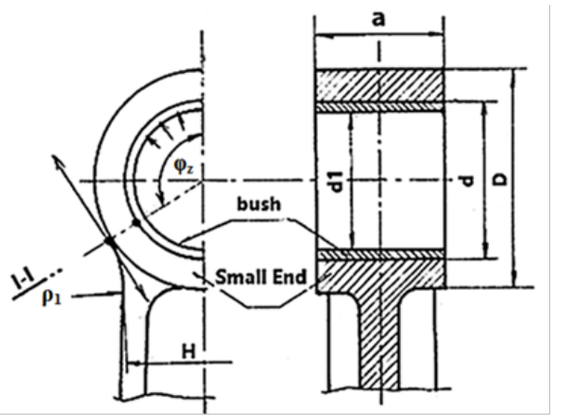

Fig. 1: Main dimensions of small end and bush

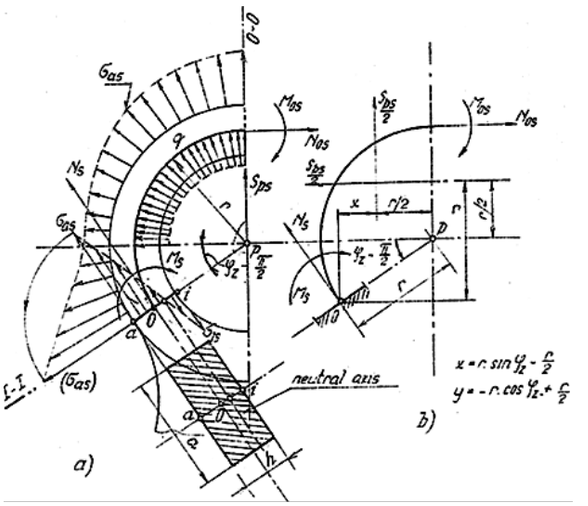

Fig. 2: Force and moment act on critical section I-I

As a case study, the external and internal stresses (σ_{ex} , σ_{in}) have been calculated for proposed moderate common values of small end dimensions and corresponding forces. It is proposed that the mean radius r = 13 mm, small end width a = 26 mm, small end thickness h = 3.5 mm, and inertia force F = 2900 N. Both internal and external stresses are calculated over a wide range of angle φ_z (from 90 to 140°). The results were blotted as shown in figure 3.

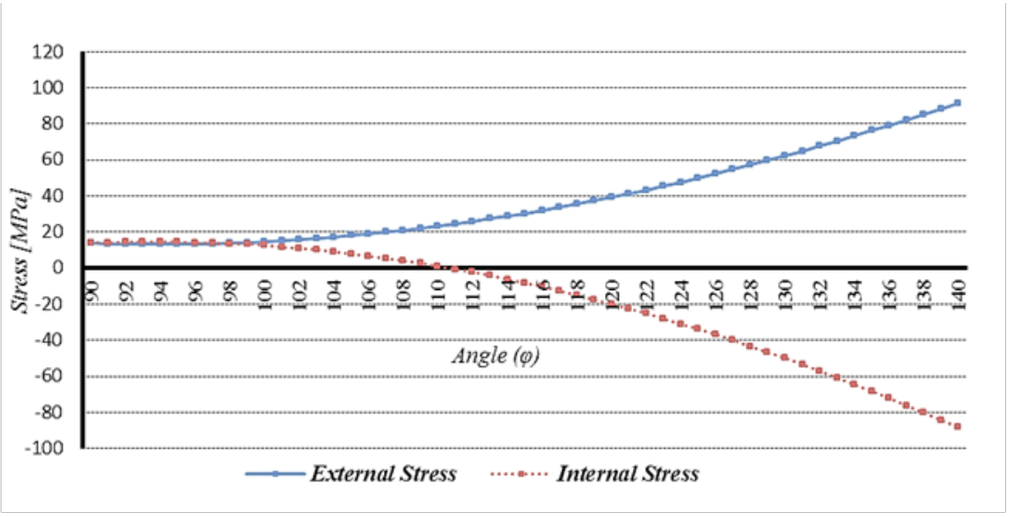

Fig. 3: External and internal stresses [MPa] for different values of angle (φz) (Case Study)

Figure 3 shows that the stresses affecting the external fiber increase as angle φz increases. While the internal stresses start with positive values at lower φ_z, and decreases to reach ZERO value at certain φ_z then increase again in negative direction. By repeating stress calculations, for different dimensions and loads, it was found that the internal stress behave the same trend, but the value of φ_{zo} at which internal stress equals zero moves back and forth depending on dimensions and loads. Figure 4 shows a sample of internal stress against different values of φ_z for different small end dimensions.

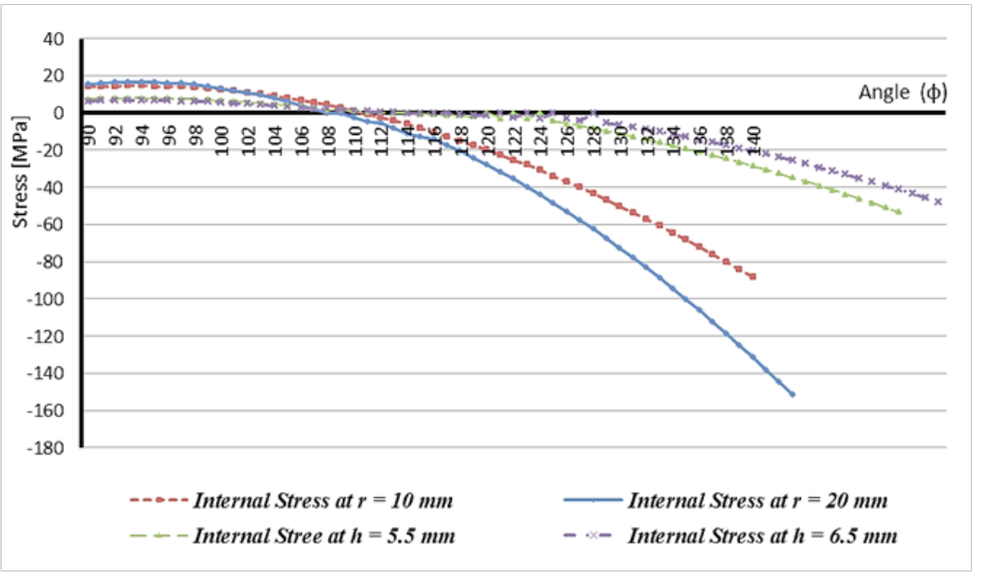

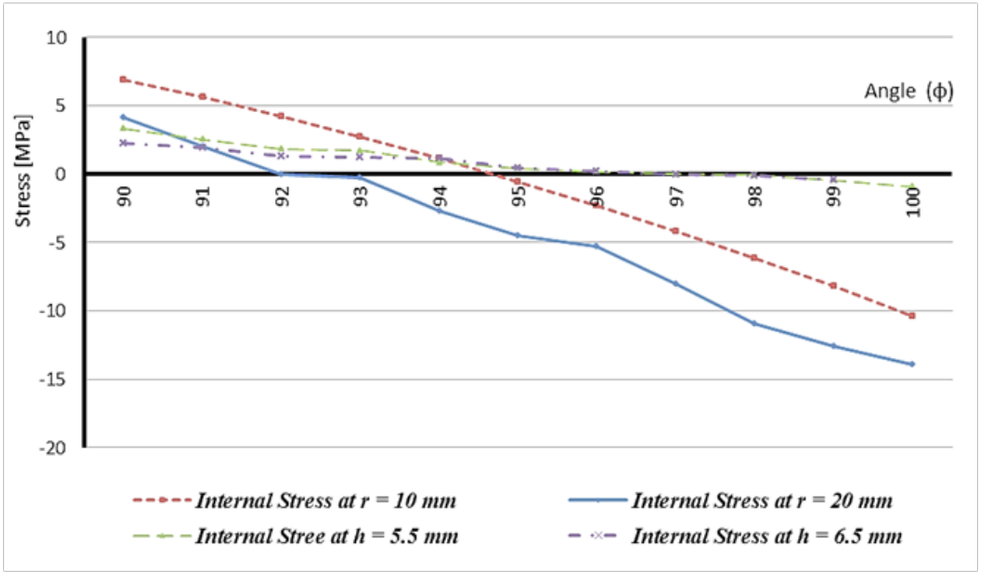

Fig. 4:. Sample of internal stresses against angle (φz) for different small end dimensions (Two Scales)

To specify the angle φ_{zo} at which internal stress equals zero, it is needed to investigate all parameters affecting it. Equation (2) shows 6 parameters that can affect φ_z, namely M_s, N_s, r, h, k, and a. So, it is required to investigate the effect of each parameter individually on φ_z while others remain constant. Both M_s and N_s can be calculated from equations (3 and 4) which are function in φz, r, and inertia force F. The question now is, how to choose previous parameters values.

It is well known that there is a wide variety in engine dimensions and sizes according to required output power and its application. In this study, the piston diameter has been chosen in range 65 to 165 mm, which corresponding to output power about 3 to 400 kW. Most of these engines run at average speed 3000 rpm, which corresponding to 600 to 10000N inertia force for masses which conduct linear reciprocating motion in engine parts. Table 1 shows typical dimensions of small end and corresponding inertia forces for different piston diameters, and at average velocity 3000 rpm.

Table 1: Typical values of small end dimensions for different cylinder bore

	Cylinder bore [mm]			
	65	96	130	165
Small end external diameter, D [mm]	23.5	34.5	45.5	56.5
Small End internal Diameter, d [mm]	16.5	25.5	34.5	43.5
Mean radius, rm [mm]	10	15	20	25
Small end thickness, h [mm]	3.5	4.5	5.5	6.5
Small end width, a [mm]	22	34	48	62
Inertia force, F [N]	575	1950	4750	10000

The inertia force can be calculated from equation (9):

$$F = m * \omega^2 * r * (1+\lambda) \qquad (9)$$

Where,

ω angular velocity
r crank radius
λ ratio of crank radius to connecting rod length
m mass which conducts linear motion and can be estimated from Figure 5.

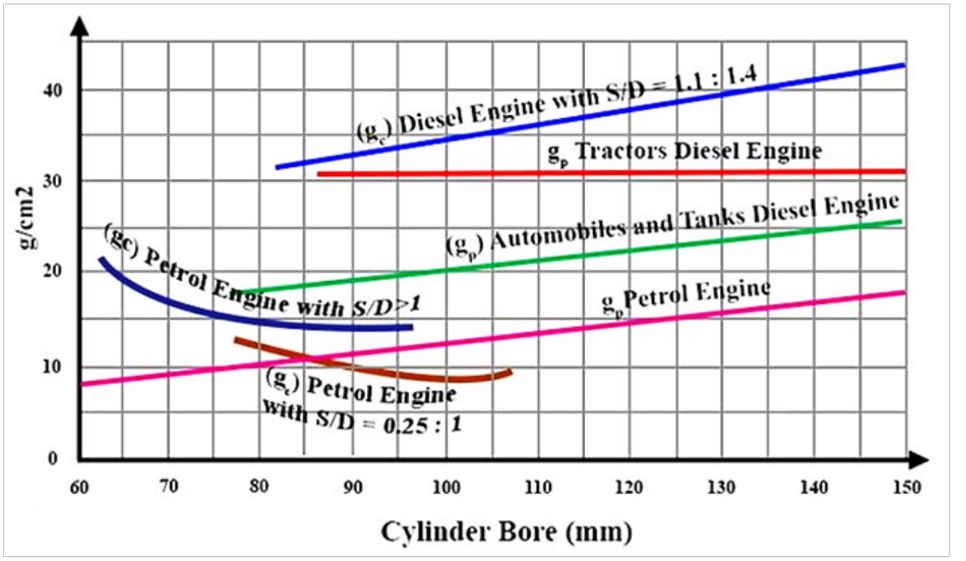

Fig. 5: Weight of piston Group (g_p) and connecting Rod (g_c) per unit piston area

First, the effect of inertia force on value of angle φ_{zo} at which internal stress equals zero, has been investigated for different small end dimensions. According to table 1, forces have been chosen from 1000 to 10000N. Results show that change of inertia force for same dimensions does not affect the value of angle φ_{zo}. Figure shows constant value of φ_{zo} (112.563° for this case dimensions) for different values of inertia force.

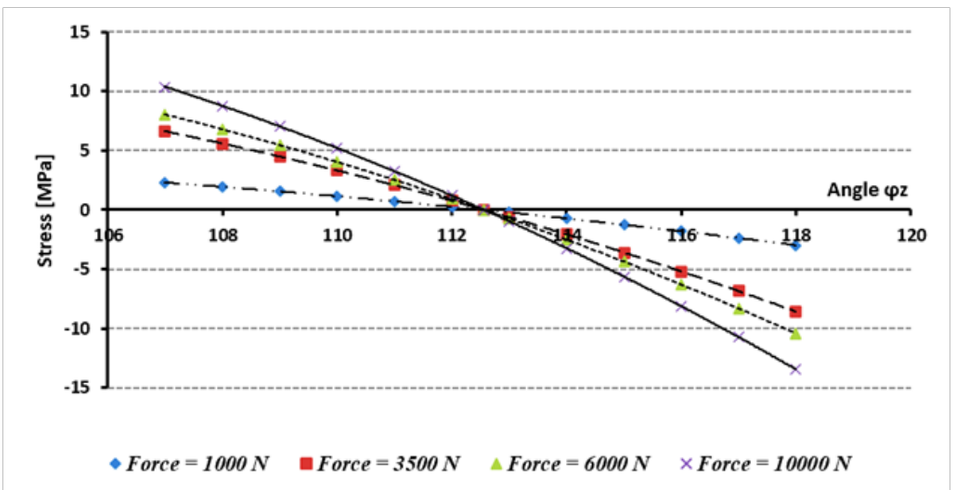

Fig. 6: Effect of applied inertia force on angle (φzo) at which the internal stress equals zero for the same small end dimensions

By studying the effect of change of mean radius (r) (from 10 to 25 mm), and small end thickness (h) (from 3.5 to 6.5 mm) as given in table (1), it was found that: the angle φ_z at which internal stress equals zero decreases as (r) increases for same (h), and increases as (h) increase for same (r), for a fixed value of stress distribution coefficient (k = 0.872), as shown in figure 7.

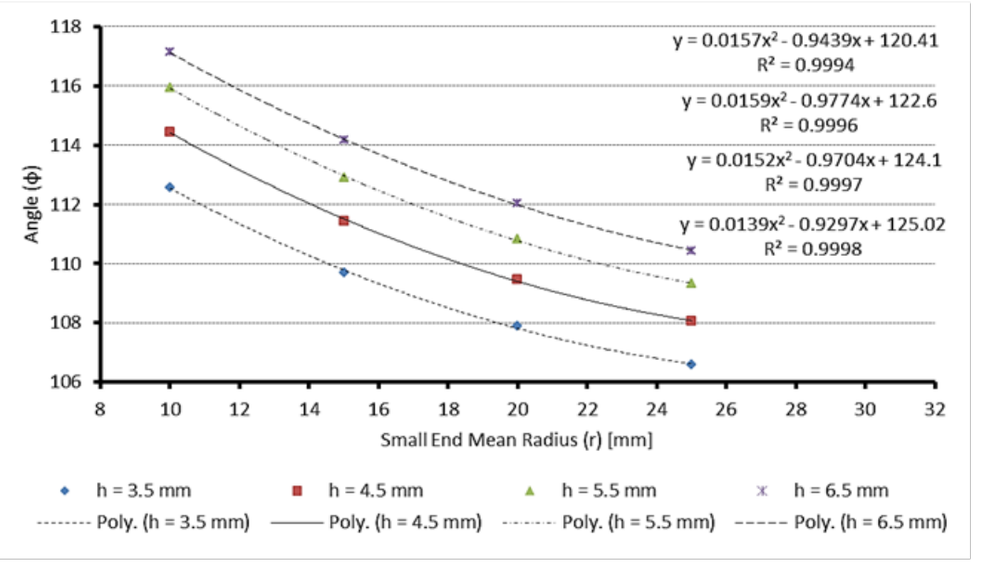

Fig. 7: Effect of mean radius (r) and small end thickness (h) on angle (φzo) at which the internal stress equals zero for the Same k =0.872

By repeating all previous calculations for different values of small end width (a = 22 to 62 mm) in factorial manner, it was found that change in width (a) does not have a significant effect on angle φ_{zo} at which internal stress equals zero.

All previous calculations have been conducted to a single value of stress distribution coefficient (k = 0.872). So, it is necessary to repeat these calculations for different values of (k). Table 2 shows values of φ_{zo} at which internal stress equals zero for different values of k, h, and r.

Table 2: Angle φ_{zo} [deg.] at which internal stress equals zerofor different values of r, h, and K

	rm [mm]	h [mm]			
		3.5	4.5	5.5	6.5
k = 0.772	10	111.537	113.312	114.73	115.858
	15	108.845	110.481	111.862	113.044
	20	107.131	108.619	109.902	111.025
	25	105.927	107.291	108.48	109.535
k = 0.872	10	112.058	113.886	115.343	116.502
	15	109.285	110.971	112.394	113.609
	20	107.516	109.051	110.373	111.531
	25	106.273	107.681	108.908	109.996
k = 0.872	10	112.563	114.439	115.935	117.123
	15	109.711	111.444	112.907	114.155
	20	107.889	109.468	110.8305	112.021
	25	106.609	108.059	109.323	110.442
k = 0.922	10	113.052	114.976	116.51	117.725
	15	110.124	111.905	113.405	114.685
	20	108.253	109.878	111.275	112.496
	25	106.936	108.428	109.726	110.875

Data in table (2) have been utilized to correlate the values of angle φ_{zo} to other small end parameters k, r, and h. Regression results and statistics, using least square method are illustrated in table 3. It is seen that R^2 = 0.978977 and Significance F = 2.9699*10-50 . The obtained relation then is:

$$\varphi_{zo}\,[\text{deg.}] = (1.39221 * h) - (0.41844 * r) + (9.44394 * k) + 103.552 \quad (9)$$

(r) and (h) are in [mm].

Table 3: Regression summary output for angle (φ_{zo}) and other parameters k, r, and h.

SUMMARY OUTPUT

Regression Statistics	
Multiple R	0.98943268
R Square	0.978977028
Adjusted R Square	0.977925879
Standard Error	0.432679968
Observations	64

ANOVA

	df	SS	MS	F	Significance F
Regression	3	523.0740911	174.3580304	931.3402586	2.96992E-50
Residual	60	11.23271729	0.187211955		
Total	63	534.3068084			

	Coefficients	Standard Error	t Stat	*P*-value	Lower 95%	Upper 95%	Lower 95.0%	Upper 95.0%
Intercept	103.5519912	0.872716139	118.6548369	6.98156E-73	101.806299	105.2976834	101.806299	105.2976834
X Variable 1	-0.418435625	0.009675018	-43.2490788	6.19792E-47	-0.437788543	-0.399082707	-0.437788543	-0.399082707
X Variable 2	1.392209375	0.048375091	28.77946779	8.20546E-37	1.295444786	1.488973964	1.295444786	1.488973964
X Variable 3	9.4439375	0.967501821	9.761157337	5.29492E-14	7.508645714	11.37922929	7.508645714	11.37922929

The maximum error between calculated (as shown in table 2) and predicted (using equation 9) values of angle (φ_{zo}) is 0.7% as shown in fig. (8). Equation 9 could be a useful tool for engine designers by using it to predict (φ_{zo}) value, then using equation (8) to specify dimensions H, ρ1, and D which achieve this value.

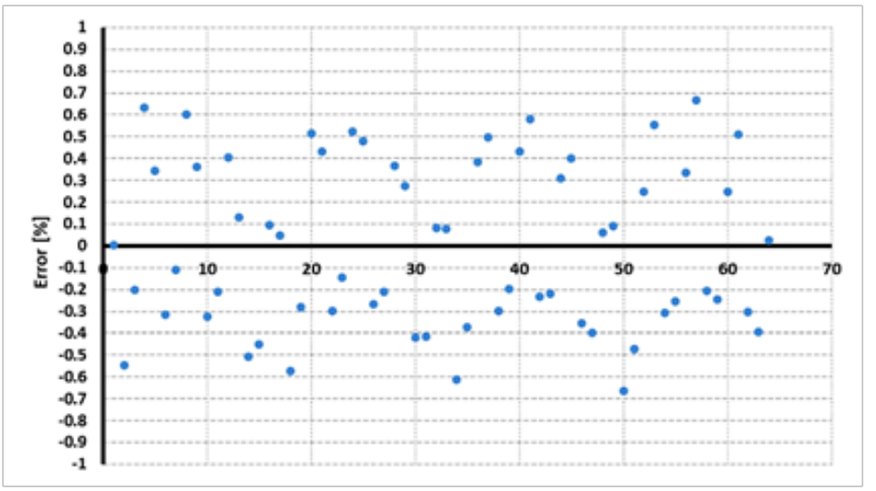

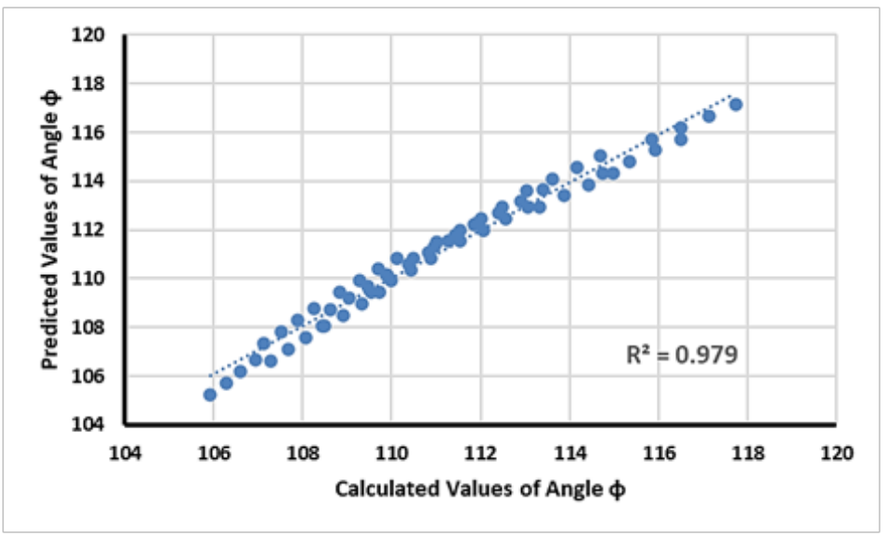

Fig. 8: Error % between Calculated and predicted Values of Angle (φ_{zo})

3. RESULTS VALIDATION

To validate the analytical equations (1 to 8) which were used as the basis for the presented parametric analysis, the results calculated by these equations have been compared to the results obtained by finite element using ANSYS software[19].

Pravardham S. Shenoy[19] conducted a comprehensive load analysis for connecting rod parts, small end, shank and big end using finite element analysis at several crank angles. Finite element mesh was generated with a uniform global element length of 1.5 mm, and at locations with chamfers a local element length of 1 mm was used, this resulted in a mesh with 104471 elements. The small end is assumed to have a sinusoidal distributed load over the contact surface area, under tensile loading, this is based on experimental results obtained from Webster *et al.* 1983[20]. Shenoy elected dimensions of the small end to be external diameter D = 30mm, internal diameter d = 20 mm, and thickness h = 5 mm as clarified in drawing in Appendix A, and uniformly distributed load of 26.7 kN was taken to be applied at the connecting rod small end.

Figure 9 shows the von Mises stress distribution with tensile load at the piston pin end, while the crank end is restrained. The same figure also shows locations of 12 nodes at which stresses are computed using ANSYS.

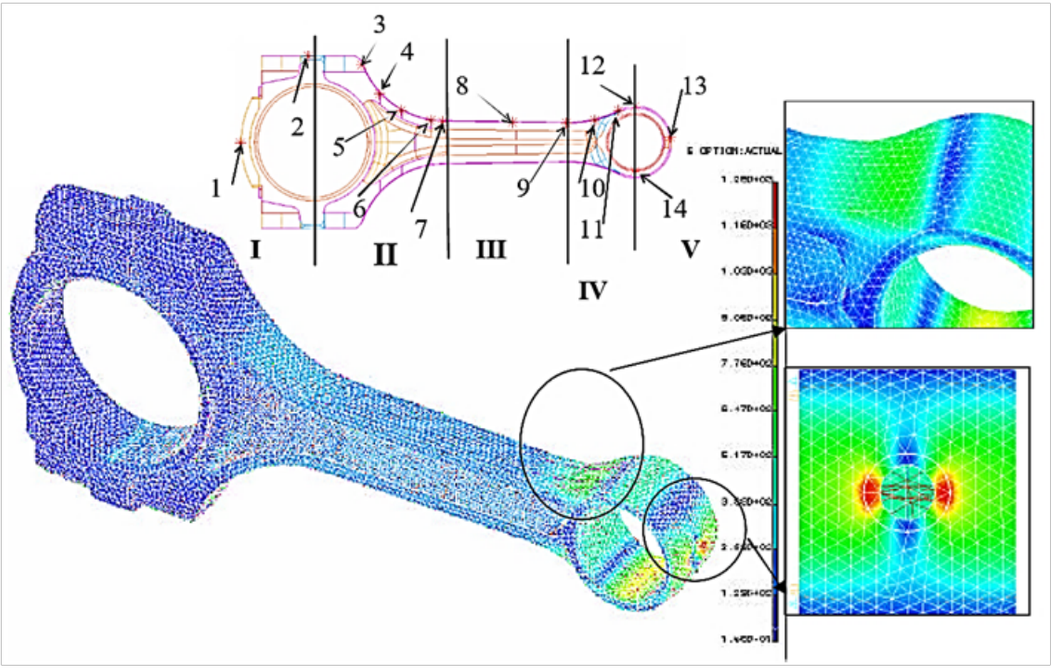

Fig. 9: Von Mises stress distribution with tensile load of 26.7 kN at small end[19]

Table 4 summarizes stress values (MPa) at different 12 locations (as shown in figure 9), for 4 cases (boundary conditions). The first case is tensile load at small end (FEM-1), the second is tensile load at big end (FEM-2), while the third is compressive load at small end (FEM-3), and the last one is compressive load at big end (FEM-4). Table 4 shows that the stress at the external fiber of small end at transition section between small end and shank (location 11 in figure 9) is 147.4 Mpa in case of small end tension (FEM-1) and previously mentioned dimensions and load.

Table 4: Comparison of static axial stresses for four FEA model boundary conditions [19].

	Region	I		II					III		IV			V	
	Node Label	1	2	3	4	5	6	7	8	9	10	11	12	13	14
Tensile load at pin end (FEM-1)	Stress (MPa)	3.3	46.2	16.8	54.1	221.5	238.9	202.7	192.8	185.3	595.9	147.4	460.3	813.9	952.6
Tensile load at crank end (FEM-2)	Stress (MPa)	465.6	211.7	30.0	108.2	319.9	241.4	200.1	196.6	196.0	355.8	55.4	186.0	4.6	443.0
Compressive load at pin end (FEM-3)	Stress (MPa)	7.3	10.5	2.2	26.2	122.1	249.1	215.4	196.5	202.9	306.7	98.0	57.8	54.0	66.7
Compressive load at crank end (FEM-4)	Stress (MPa)	32.2	26.1	10.3	11.8	175.2	251.4	212.3	196.5	204.7	147.2	11.0	7.7	3.3	8.0

Now, equations (1 to 8) can be used to predict the stress acting on the small end external fiber for the same dimensions and load which were introduced by Pravardham S. Shenoy. Where mean radius rm is 12.5 mm, small end thickness h = 5 mm, width = 20 mm, shank section width H = 18 mm, and curvature ρ = 90 mm as shown in appendix A.

First, equation 8 is used to calculate the angle at which the critical transition section is located ϕ_z = 109.46o in this case, then equations (1 to 6) are used to calculate the

stresses acting on external and internal fibers of small end. Table 5 shows the calculated results for equations (1 to 6) at different values of transition angle ϕ_z (from 107 to 114).At angle 109.46o , the calculated external stress (σ_{ex}) is 149.51 MPa, which is very close to that predicted one by ANSYS (147.4 MPa) with error 1.43%, which confirms the validity of these equations and obtained results.

Table 5: Calculated external and internal stresses for different angles ϕ_z, using equations 1 – 6.

Angle (Φz)		Mos [N.m]	Nos [N]	Ms [N.m]	Ns [N]	σex [Mpa]	σin [Mpa]
Degree	Radian						
107	1.868253968	1.797444	12986.88	3.314829947	12870.158	134.7158059	52.95000053
108	1.885714286	1.903176	12965.52	3.891666567	12812.55919	140.424067	44.42962498
109	1.903174603	2.008908	12944.16	4.510061399	12751.76358	146.5509365	35.30275529
109.46	1.911206349	2.05754472	12934.3344	4.808427116	12722.72806	149.5093499	30.90148102
110	1.920634921	2.11464	12922.8	5.169827343	12687.78559	153.0945297	25.57212194
111	1.938095238	2.220372	12901.44	5.870767484	12620.64035	160.0528633	15.2405987
112	1.955555556	2.326104	12880.08	6.61267513	12550.34376	167.4238552	4.311202007
112.57	1.965507937	2.38637124	12867.9048	7.053810839	12508.87098	171.809133	-2.184867744
113	1.973015873	2.431836	12858.72	7.395333857	12476.91247	175.2053254	-7.212909715
114	1.99047619	2.537568	12837.36	8.218517562	12400.36388	183.3949965	-19.32843671

4. CONCLUSION

Connecting rod small end is subjected to stress acting on its external and internal fibers. These stresses result from inertia force of piston group mass. The transient section between small end and shank is considered as the most critical section. This section is at angle φ_z, this angle depends on small end and shank dimensions. The value of the stress on the internal fibers is found to be zero at certain value of φ_z.

In this work, a comprehensive investigation has been conducted to study the effect of changing small end design parameters on the value of angle (φ_{zo}) at which the stress on the internal fibers diminishes. It was concluded that:

• Changing the value of inertia force (F) and small end width (a) does not affect the value of (φ_{zo}).

• Small end thickness (h), mean radius (r), and load distribution factor (k) have dominant effect on (φ_{zo}) value.

• By using regression, a new relation between (φzo) and dominant design parameters has been introduced. The error between predicted and calculated values of (φ_{zo}) did not exceed 0.7%.

• Verification of the analytical parametric analysis has been conducted by comparing its results to obtained numerical analysis results using ANSYS finite element software, the error is 1.43%.

• Such a correlation could be a useful tool for engine designers to predict the value of (φ_{zo}) as a guide for choosing the small end dimensions and materialin order to minimize the connecting rod weight and price.

5. REFERENCES

[1] M. Khovakh 1979 Motor Vehicle Engines", MIR Publisher, Mosco
[2] Vivek C. Pathade, and Dilip S. Ingole 2013 Stress analysis of I.C. engine connecting rod by FEM and photoelasticity,IOSR-JMCE ISSN 2278-1684,Vol 6, Issue 1, 2013, pp 117-125.
[3] Akbar H. Khan and Dhananjay R. Dolas 2017 Static structural and experimental stress analysis of connecting rod using FEA and Photoelasticity,IJIRSET ISSN 2319-8753,Vol 6, Issue 1, pp 578-585.
[4] Shriram A. Phad and D.H. Burande 2013 Static and dynamic analysis of connecting rod of compressor, IJAnERD ISSN 2277-4785,Vol 3, Issue 3, pp 23-30.
[5] B.Anusha,C.Vijaya, andBhaskarReddy 2013 Comparison ofmaterials fortwo-wheeler connecting rod using Ansys, International Journal of Engineering Trends and Technology, Volume 4, Issue 9, Sep.
[6] Abhinav Gautam, and K PriyaAjit 2013 Static stress analysis of connecting rod using finite elementapproach, IOSR Journal of Mechanical and Civil Engineering, Volume 10, Issue 1, Nov. , PP 47-5.
[7] Pushpendra Kumar Sharma, and Borse Rajendra R. 2012 Fatigue analysis and optimization of connecting rod using finite element analysis, IJARSE ISSN 2319-8354,Vol 1, Issue 1.
[8] Nilam Pranjal Patil Dhande, Pundlik Patil, and R.Y. Patil, 2018 Analysis of connecting rod for weight reduction in case of a CI engine, IJEDR, Volume 6, Issue 1,
[9] Magesh Kumar, and Ankush K Biradar, 2017 Design, analysis and optimization of connecting rod, International Journal of Innovative Research in Science, Engineering and Technology, Volume 6, Special Issue 11.
[10] N. A. Wankhade, and Suchita Ingale 2017 Review on design and analysis of connecting rod using different material, International Journal of Engineering Science and Computing, Volume 7.
[11] Mithilesh K Lade, Ritesh P Harode, and DeepaliBankar Lade 2015 Static load analysis of carbon fiber connecting rod,International Journal of Research in Advent Technology, Volume 3, No.9.
[12] Adnan Ali Haider, Akash Kumar, AjinkyaChowdhury, Moin Khan, and P. Suresh 2018 Design and structural analysis of connecting rod, International Research Journal of Engineering and Technology (IRJET), Volume: 05, Issue: 05.
[13] A. Strozzi, A. Baldini, M. Giacopini, E. Bertocchi, and S. Mantovani 2016 A repertoire of failures in connecting rods for internal

combustion engines, and indications on traditional and advanced design methods,Engineering Failure Analysis 60, 20-39.
[14] Sharma Manoj, and Shashikant 2015 Optimization of connecting rod with help of FEA,IJMET ISSN 0976-6359,Vol 6, Issue 7, pp 51-57.
[15] B. K. Roy 2012 Design analysis and optimization of various parameters of connecting rod using CAE software, IJNIET, Volume 1, Issue 1.
[16] Nilam P. Patil, Pundlik N. Patil, Raghunath, and Y. Patil 2017 Design analysis of connecting rod for weight Reduction in case of a CI Engine – A Review", International Journal of Engineering Sciences and Research Technology.
Mansi S. Satbhai, and P.S. Talmale 2017 Review on design and analysis of two-wheelerconnecting rod, International Research Journal of Engineering and Technology, Volume: 04, Issue: 09.
[18] Lingaraj K. Ritti, Pavan Kumar, and AmbarishM. 2015 Size and shape optimization of a two-wheelerconnecting rod by structural analysis, International Journal of Analytical, Experimental and Finite Element Analysis, Volume 2, Issue 1.
[19] Pravardhan S. Shenoy, May 2004, Dynamic load analysis and optimization of connecting rod, Master of Science thesis in Mechanical Engineering, University of Toledo,Ohio, USA.
[20] Webster, W. D., Coffell R., and Alfaro D., 1983, A three-dimensionalfinite element analysis of a high speed diesel engine connecting rod, SAE Technical Paper Series, Paper No. 831322.

Appendix A:

Connecting rod dimensions as studied by[19]